Numerical Simulation of the 1993 Midwestern Flood: Land–Atmosphere Interactions

MICHAEL G. BOSILOVICH* AND WEN-YIH SUN

Department of Earth and Atmospheric Science, Purdue University, West Lafayette, Indiana

(Manuscript received 23 July 1997, in final form 24 June 1998)

ABSTRACT

During the summer of 1993, persistent and heavy precipitation caused a long-lived, catastrophic flood in the midwestern United States. In this paper, Midwest hydrology, atmospheric circulation of the 1993 summer, and feedback between the surface and precipitating systems were investigated using the Purdue Regional Model (PRM). The 30-day PRM control simulations reproduced the large-scale atmospheric features that characterized the summer of 1993. Specifically, the upper-level jet stream and trough over the northwestern United States are present in control cases, as well as the Great Plains low-level jet, general pattern of moisture transport, and heavy precipitation in the Midwest. The daily precipitation record (area averaged over the heaviest rainfall) indicates that the model also reproduces the evolution and periodicity of precipitation events comparable with the observations and correctly depicts the differences between June and July.

The sensitivity of the low-level jet, planetary boundary layer, and heavy precipitation were examined by imposing various soil moisture and surface anomalies in the model simulation. The increased surface heating, caused by a strong dry anomaly, induced a large-scale surface pressure perturbation, centered in the southeastern United States, that weakened the low-level jet and moisture convergence within the flood region. Separate cases considering both wet and dry regional anomalies in the southern Great Plains caused less precipitation in the flood region. The uniform soil moisture of both anomalies leads to a reduction of the differential heating, surface pressure gradient, and the low-level jet.

1. Introduction

In the spring of 1993, heavy precipitation in the Mississippi River basin saturated the soil. During the subsequent summer, record amounts of precipitation fell in regions where the soil was moist from the spring rain and led to sustained flooding along the Mississippi River (Kunkel et al. 1994). The correlation between saturated soil moisture and subsequent increased precipitation suggests that local evaporation sustained by large soil moisture helped to enhance local precipitation, a process called recirculation of water (Mintz 1984; Betts et al. 1994; Trenberth and Guillemot 1996). Mesoscale processes related to the planetary boundary layer and surface soil moisture, however, could also have contributed to the heavy precipitation (Beljaars et al. 1996; Paegle et al. 1996; Giorgi et al. 1996), and the actual degree of recycling is not well quantified.

Lower-tropospheric flow during the summer in the central United States is normally from the south, and tropical air masses around the Gulf of Mexico provide significant amounts of moisture for precipitation (Roads et al. 1994; Min and Schubert 1997; and many others). Bell and Janowiak (1995) and Mo et al. (1995) have discussed large-scale aspects of the anomalous atmospheric circulation during the flood of 1993. In general, an upper-level trough was centered over the northwestern United States, with strong upper-level divergence downstream over the midwestern United States. The upper-level jet stream was much stronger than normal, and extended into the midwestern United States (hereafter called the Midwest), much farther south than normal. During the summer of 1993, the low-level wind was much stronger than normal, leading to increased atmospheric moisture transport into the Midwest. This combination of upper- and lower-tropospheric circulations is generally thought to be conducive to intense mesoscale convection in the United States (Maddox 1983; Kunkel et al. 1994; Bell and Janowiak 1995). This situation is remarkably similar to the strong low-level jet cases studied by Uccellini (1980) and Chen and Kpaeyeh (1993).

Both Mo et al. (1995) and Bell and Janowiak (1995) demonstrated some features of intraseasonal variability during the 1993 summer. During June, a series of synoptic-scale cyclone systems propagated across the

* Current affiliation: Universities Space Research Association, NASA/Goddard Space Flight Center, Greenbelt, Maryland.

Corresponding author address: Dr. Michael G. Bosilovich, Universities Space Research Association, Code 910.3, NASA/Goddard Space Flight Center, Greenbelt, MD 20771.
E-mail: mikeb@dao.gsfc.nasa.gov

Rocky Mountains and into the Midwest, following a track that was much farther south than usual. These cyclones were the primary cause of the precipitation in June. The large-scale circulation during July, however, became much more stationary and exhibited the features discussed above, providing an environment favorable for mesoscale convection.

The importance of land surface processes in precipitating systems and regional climate has been known for quite some time. For example, Mintz (1984) found that, for normal summer months in the United States, surface evaporation was the main determinant of precipitation. In this argument, it is assumed that convective precipitation draws water vapor from the planetary boundary layer, and that the magnitude of evapotranspiration is assumed to be an order of magnitude greater than the large-scale moisture convergence. Some midlatitude convective systems, however, form in conjunction with significant horizontal transport and convergence of moisture (e.g., Maddox 1983). Along these lines, it has been suggested that, because the surface soil water was much above normal levels, the surface evaporation was the source of much of the summer 1993 precipitation (Betts et al. 1994; Trenberth and Guillemot 1996). On the other hand, potential evapotranspiration, was below normal, due to increased cloud cover, lower surface temperature, and higher surface-layer specific humidity (Kunkel et al. 1994). Furthermore, the climatologic summer actual evapotranspiration of the Mississippi River basin is between 3 and 4 mm day^{-1} (Roads et al. 1994), while the 1993 evapotranspiration may not be much larger than climatology (4 mm day^{-1}; Trenberth and Guillemot 1996).

Recently, some numerical modeling studies have tested the sensitivity of the 1993 atmospheric circulation to surface evaporation. Beljaars et al. (1996) found that, in 1993, dry soil greatly reduced the amount of precipitation by causing a strong inversion at the top of the planetary boundary layer (PBL) that limited the development of deep convection. In contrast, Paegle et al. (1996) found that wet soil reduced the diurnal heating of the PBL and the diurnal oscillation of the low-level jet (LLJ), leading to a reduction of moisture convergence and precipitation. McCorkle (1988) and Sun and Wu (1992) found that differential surface heating in the southern Great Plains can enhance the LLJ. In testing similar cases, the results of Giorgi et al. (1996) compared well with those of Paegle et al. (1996); however, subsequent experiments employing larger model domains were found to compare more favorably with those of Beljaars et al. (1996) (Seth and Giorgi 1997).

In this paper, Purdue Regional Model (PRM) numerical simulations of the 1993 Midwestern floods are presented and the model's sensitivity to land surface and planetary boundary layer processes are examined. The following section outlines the numerical simulations and experimentation. Section 3 presents the model representation of the atmospheric circulation and its comparison to observations. Finally, the interaction between the model surface, boundary layer, and precipitation are discussed in the context of sensitivity experiments.

2. Model and methodology

The PRM has been developed over the past 12 years at Purdue University and has been used for a wide range of space and timescales for atmospheric numerical simulation. Chern (1994) provides a complete summary of the current PRM physics and numerical formulation, while Sun and Yildirim (1989), Sun and Chern (1993), Sun et al. (1991), Hsu and Sun (1991, 1994), and Sun and Wu (1992) discuss several developmental stages of the PRM. Given the large resource of information available regarding the model, only a brief review is presented here.

The PRM is a hydrostatic primitive equation model that utilizes the terrain-following normalized pressure coordinate (σ_p) in the vertical direction. The model's horizontal grid is the staggered (Arakawa C) grid, which permits more accurate computation of the mass divergence during the model simulation. The atmospheric model has prognostic equations for momentum, heat, turbulent kinetic energy (TKE), surface pressure, and all phases of water. The model thermodynamic variable is the equivalent ice potential temperature. Significant effort has been made to ensure the accuracy of the numerical methods used to solve the governing equations. A new method of computing the pressure gradient force in the momentum equations greatly reduces the truncation error near complex topography (Sun 1995). Horizontal advection is computed using a combination of the Crowley fourth-order advection scheme and the Gadd advection scheme (Sun 1993a). Sun and Wu (1992) describe the atmospheric radiation parameterization in detail, and the cumulus parameterization is a Kuo-type scheme (Molinari 1982).

The PBL parameterization is a 1.5-order closure scheme that includes TKE as a prognostic variable (see Sun 1993b) and has provided remarkable results for many different PBL experiments. Sun (1993b) showed that the model could predict the convective PBL and the development of a nocturnal LLJ during the Wangara Experiment. In addition, the model has been applied successfully to the simulation of plumes released from a point source at several vertical levels in the PBL (Sun and Chang 1986a,b), the simulation of mesoscale airmass modification over Lake Michigan (Sun and Yildirim 1989), the simulation of airflow over complex terrain (Sun and Chern 1993, 1994), the formation and diurnal movement of the west Texas dryline (Sun and Wu 1992), and the sensitivity of convective PBL development to variations in the land surface (Sun and Bosilovich 1996).

The PRM uses the land surface parameterization (LSP) developed by Bosilovich and Sun (1995). Diffusion equations predict the heat and moisture within

the soil (Philip 1957; Sellers et al. 1986). Because data for soil properties and initialization are still limited, only three model layers are included in the soil, but this may be sufficient for the present purposes (Bosilovich and Sun 1998). The LSP also considers the presence of vegetation above the soil (broad leaf approximation, Deardorff 1978) including biophysical resistance to the release of water. Transpiration and evaporation of liquid water (either intercepted precipitation or dew formation) from the surface of the vegetation are both included in the model. The LSP has been verified for several short-term and long-term case studies (Bosilovich and Sun 1995, 1998).

In this study, the model simulations of June and July are first compared to observations in order to identify the veracity of the PRM and the reproduction of the different large-scale environments. Sensitivity simulations similar to those of Beljaars et al. (1996) and Paegle et al. (1996) have been reproduced using the PRM in order to identify any similarities or differences in the PBL processes discussed by these studies. Some limitations of these experiments, however, must be discussed. Because the sensitivity of the atmospheric system is in question, it is beneficial to minimize the forcing by the lateral boundaries on the region of interest (Jones et al. 1995). This is accomplished by increasing the domain size. A smaller domain or nudging the interior of the model domain may provide some improvement in the simulation, but the sensitivity will be compromised.

To study the atmospheric circulation, hydrology budget, and land surface interactions during the 1993 flood in the Midwest, the PRM is utilized. The PRM is initialized on 1 June 1993 and 1 July 1993, with European Centre for Medium-Range Weather Forecasts (ECMWF) operational analyses, and each simulation is integrated for a period of 30 days. These two months are considered separately due to the different dynamical processes that occurred during each month. The lateral boundary conditions are 6-h ECMWF operational analyses.

The model domain is presented in Fig. 1. The domain was chosen to best capture the important meteorological features of the 1993 flood, that is, to the west, the anomalous upper-level trough over the Pacific Northwest; to the north, the anomalous midwestern storm track; to the south, the easterly flow that feeds the LLJ. The eastern boundary is located far enough east so that any mismatch between the model-simulated wave pattern and the outflow boundary are far from the region of interest. Within the model interior domain (denoted by the large dark box), there is no forcing or nudging by the observations. In the region between the box and the outermost point, observations and model data are both used in the prediction of atmospheric variables. The weighting influence of the observations on the prediction decreases exponentially toward the interior box (Davies 1976).

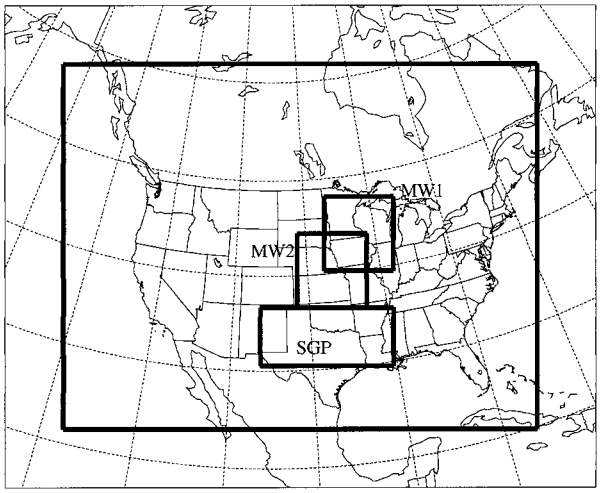

FIG. 1. The PRM domain. The large box denotes the boundary between the model interior region and area where forcing from the observational analyses is provided.

3. Control simulation verification

A crucial part of this study is the model comparison with summer 1993 observations during the flood. There are several key features that the model should reproduce, including the heavy Midwest precipitation, upper- and lower-level jets, atmospheric moisture transport, and differences between June and July atmospheric circulations. The ECMWF operational analyses that provide the initial and lateral boundary conditions are also utilized to verify the atmospheric circulation, and the National Climatic Data Center (NCDC) hourly precipitation observations (TD-3240) are compared with the PRM simulation.

a. Atmospheric circulation

As discussed earlier, the upper-level jet stream, a key feature in the anomalous atmospheric circulation, was displaced much farther south than normal during the summer of 1993. Figures 2a and 2b compare the ECMWF operational analysis and PRM simulation of the June 1993 upper-level jet stream. While the model has reproduced the general location and pattern of the jet stream, the magnitude of the core is about 2–3 m s^{-1} less than observed. Note that the modeled westerly flow in the southernmost part of the domain is stronger than observed. The model monthly mean 500-mb height fields show nearly zonal flow over the central and eastern United States, and a slight trough over the western United States, similar to observations [figure not shown, however; a more detailed comparison can be found in Bosilovich (1997)]. The June 850-mb wind speed and general patterns are very well simulated, including the LLJ over the southern Great Plains and the easterly flow over the Gulf of Mexico (Figs. 2c,d).

The 850-mb specific humidity field is also simulated

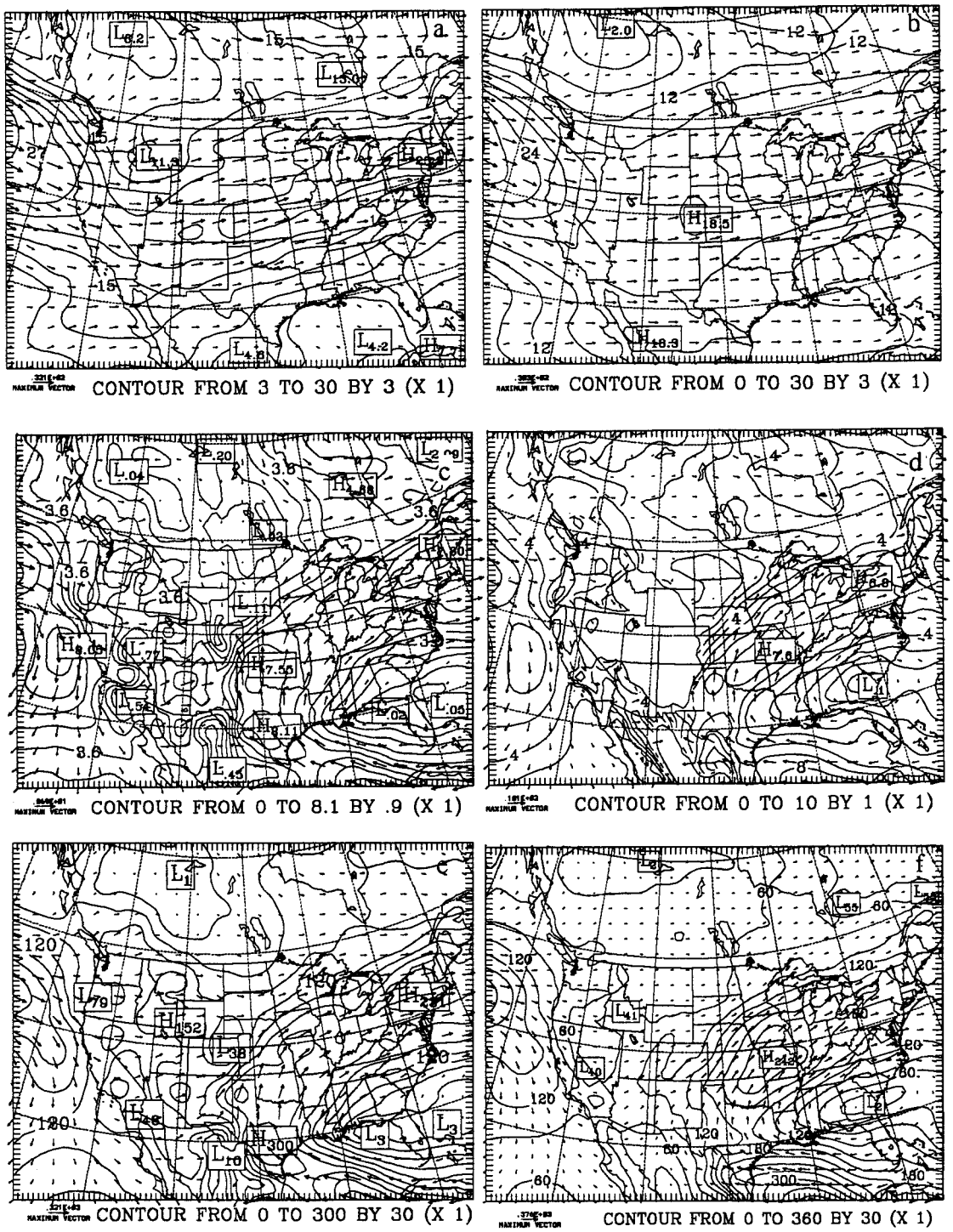

FIG. 2. June 1993 monthly mean comparison of 300-mb wind velocity (interval 3 m s^{-1}) for (a) ECMWF analyses and (b) PRM, 850-mb wind velocity (interval 1 m s^{-1}) for (c) ECMWF analyses and (d) PRM, and vertically integrated moisture transport (interval 30 kg m^{-1} s^{-1}) for (e) ECMWF analyses and (f) PRM.

well, with large specific humidity in the central United States, and lower specific humidity over the Gulf of Mexico (figure not shown). The magnitude of specific humidity, however, is generally ~0.5 g kg^{-1} lower than observed (averaged over the model interior domain). The model simulation of June mean moisture transport, both in magnitude and direction, is quite comparable to observations in the Midwest (Figs. 2e,f), although the observations

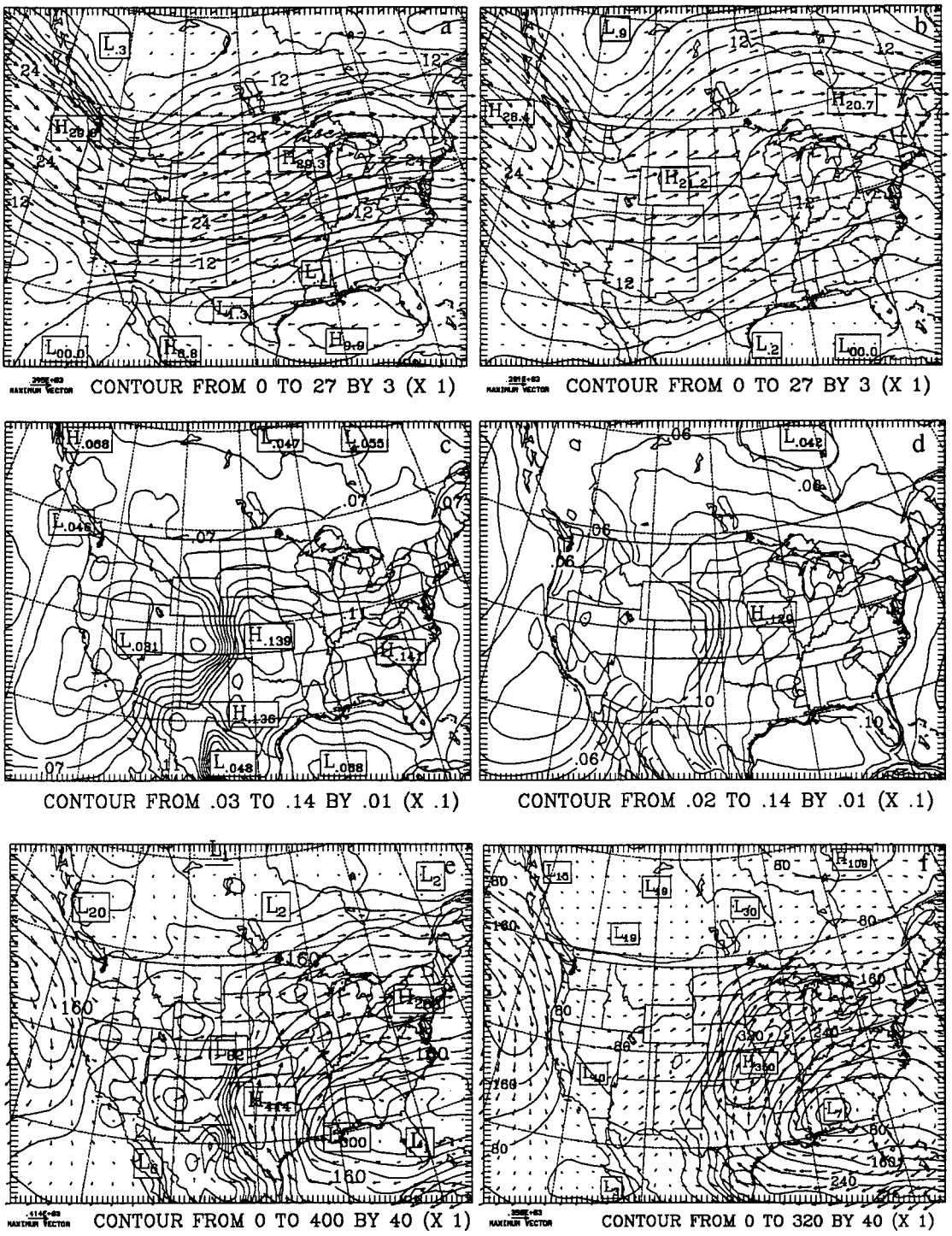

FIG. 3. July 1993 monthly mean comparison of 300-mb wind velocity (interval 3 m s^{-1}) for (a) ECMWF analyses and (b) PRM, 850-mb specific humidity (interval 0.001 kg kg^{-1}) for (c) ECMWF analyses and (d) PRM, and vertically integrated moisture transport (interval 40 kg m^{-1} s^{-1}) for (e) ECMWF analyses and (f) PRM.

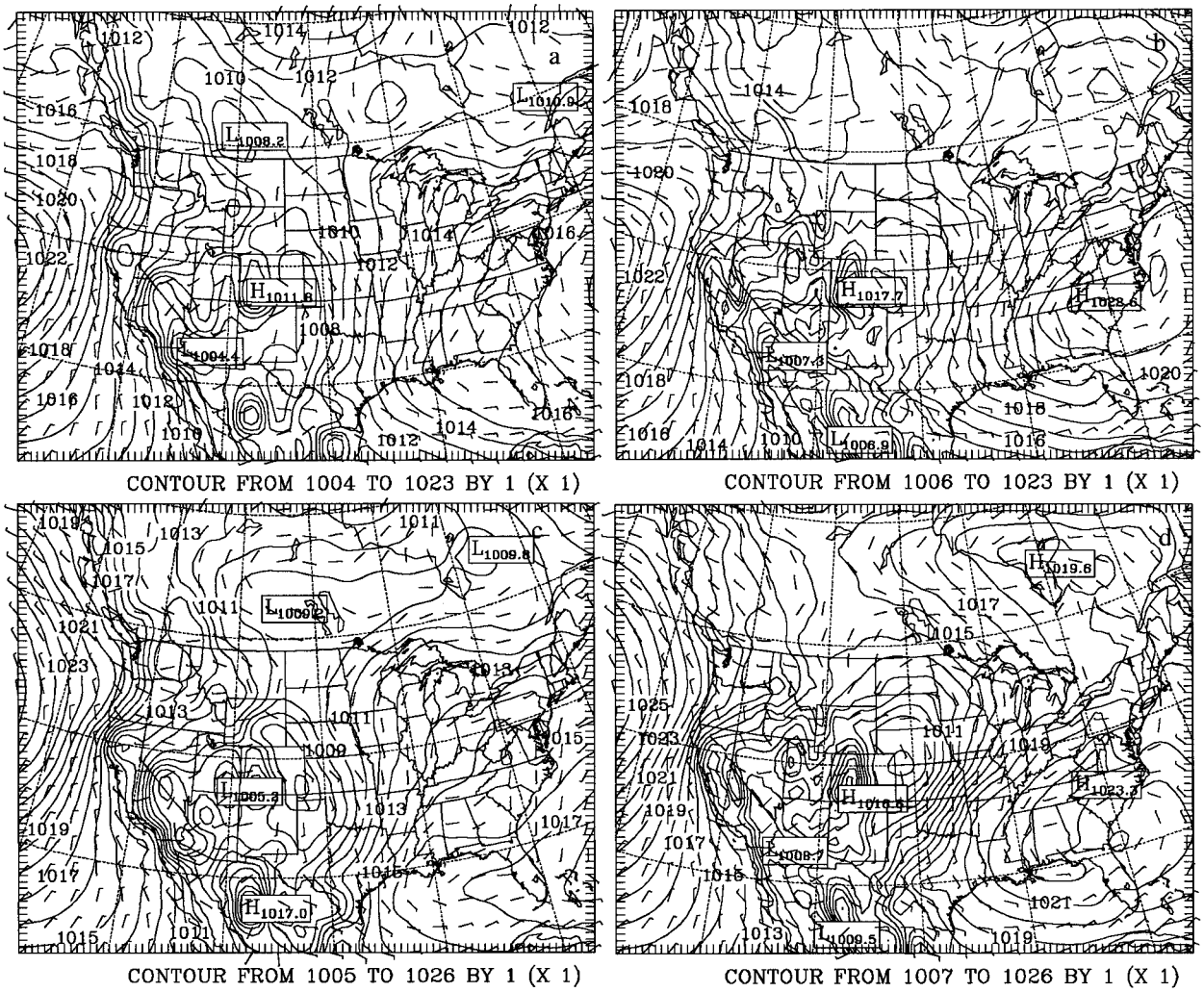

FIG. 4. Mean sea level pressure for Jun monthly mean (a) ECMWF analyses and (b) PRM simulations, and the Jul monthly mean (c) ECMWF analyses and (d) PRM simulations. The contour interval is 2 mb.

show a maximum of atmospheric moisture transport in southern Texas, which the PRM did not reproduce. Overall, the monthly mean atmospheric circulation in June appears to be realistically reproduced by the PRM.

In July, the observed longwave circulation is not as zonal as in June. While the PRM simulation of the July trough and ridge seems reasonable, the model-simulated upper-level jet stream is farther north than observed (Figs. 3a,b), especially in the Midwest region, where the heavy precipitation occurred. Also, the velocity of the wind in the jet core is again underestimated, and the upper-level easterly flow over the Gulf of Mexico is not reproduced. The July LLJ is stronger than during June in both the model and analyses, and the simulated jet is shifted north compared to the analyses (figure not shown). Higher pressure in the southeastern United States, discussed in the next section, may increase the pressure gradient and LLJ.

The model-simulated specific humidity shows a maximum over the central United States, which is comparable to the observed specific humidity during July (Figs. 3c,d). Overall, the specific humidity in the model is slightly underestimated, but especially in the southeast United States where the Bermuda high dominates. This is related to an underestimate of radiative heating and cold bias in the lower troposphere. The general pattern of atmospheric moisture transport is similar to the observations (Figs. 3e,f). Given the previous discussion of the July atmospheric circulation, it is not surprising that the maximum of atmospheric moisture transport is also shifted northward. While this discrepancy is unfortunate, the correlation of the upper- and lower-level jets and the longwave patterns in both model and observations indicates that the model does indeed reproduce the major atmospheric features responsible for the heavy precipitation.

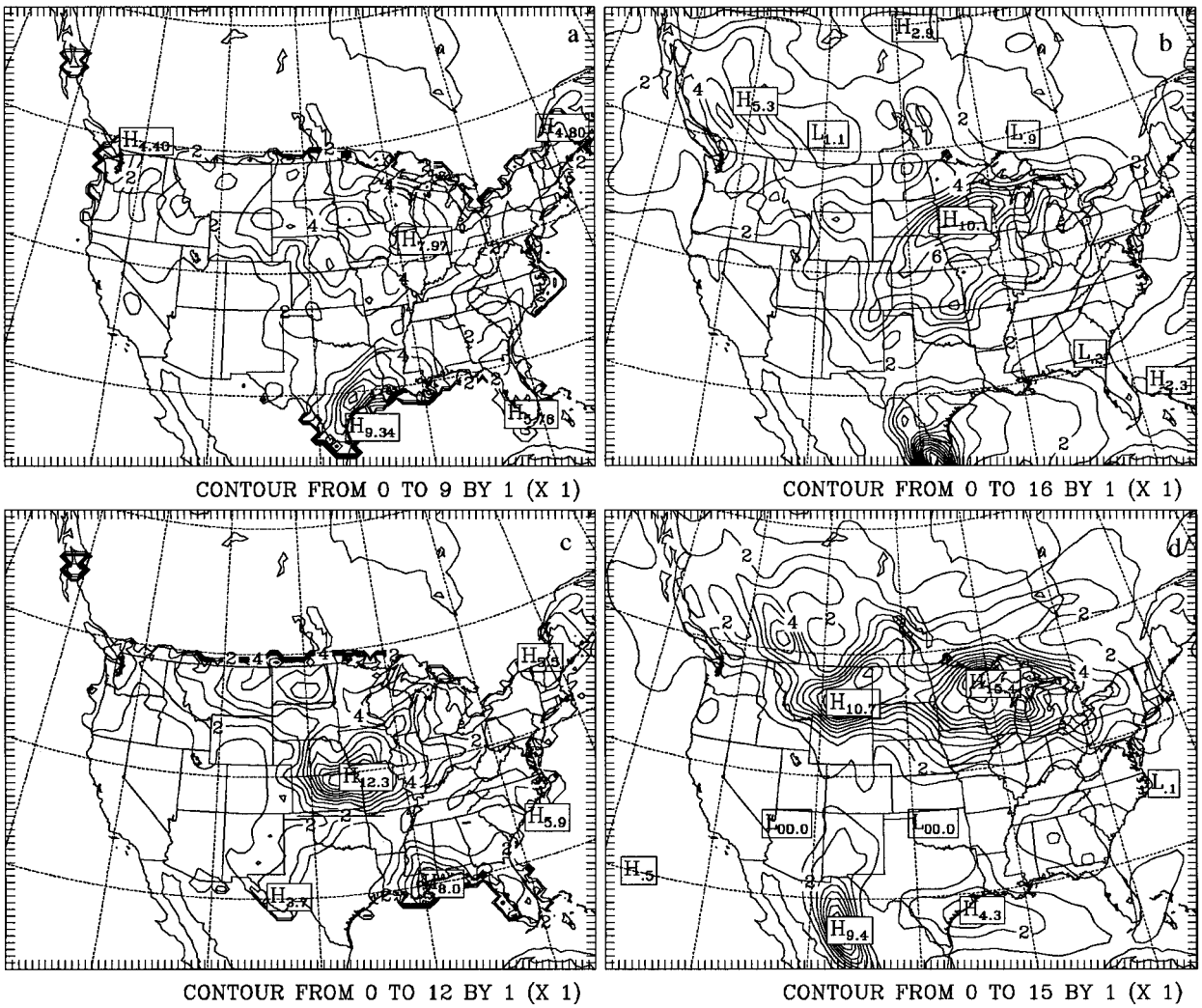

FIG. 5. Total precipitation (interval mm day^{-1}) for (a) Jun NCDC observations, (b) Jun PRM simulation, (c) Jul NCDC observations, and (d) Jul PRM simulation.

b. Surface pressure and precipitation

Figures 4a–d show the monthly mean sea level pressure and surface layer wind for June and July. In both months, the model produces low surface pressure in the lee of the Rocky Mountains. The PRM pressure fields are similar to the analyses, with the exception that the high pressure in the southeastern United States is larger than observed. The general high pressure bias in the PRM appears to be related to the model's cold temperature bias, which is caused by well-known inadequacies in the parameterization of radiation. It should be noted that, during the summer of 1993, the observed surface pressure in the lee of the Rockies was lower than normal and may have contributed to the intensification of the LLJ (Bell and Janowiak 1995).

The PRM simulated precipitation in June (Fig. 5b) shows a large area of high precipitation that is generally centered on Iowa. While this is comparable to the observed June precipitation, the model's maximum of precipitation is larger than the observed maximum. In July, however, the model's maximum of precipitation is located near central Minnesota and Wisconsin, north of the observed maximum (Figs. 5c and 5d). The location of simulated precipitation is expected because of the northward displacement of the simulated upper-level jet stream and the low-level moisture transport. Similarly, the Beljaars et al. (1996) 30-day GCM simulation also produced more precipitation north of the observed location. Precipitation amounts in July are also larger than observed. In July, the model produces a secondary maximum of precipitation in North Dakota and Montana, which is similar to observations. The model also underestimates the Gulf of Mexico coastal precipitation, which is most likely related to the land–sea breeze. The simulated July precipitation is approximately 30% larger than the observation (area averaged over the respec-

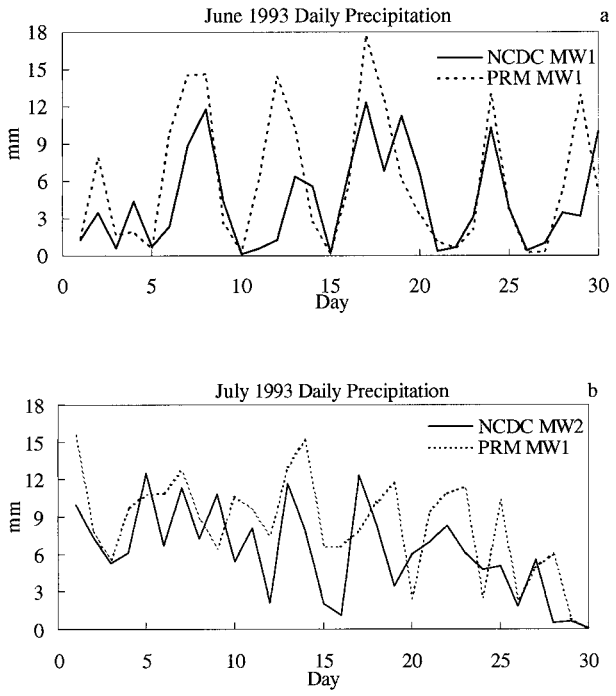

FIG. 6. PRM and NCDC observations of daily integrated precipitation (mm) for (a) Jun and (b) Jul 1993. The data are averaged over the regions noted in each graph (see Fig. 1).

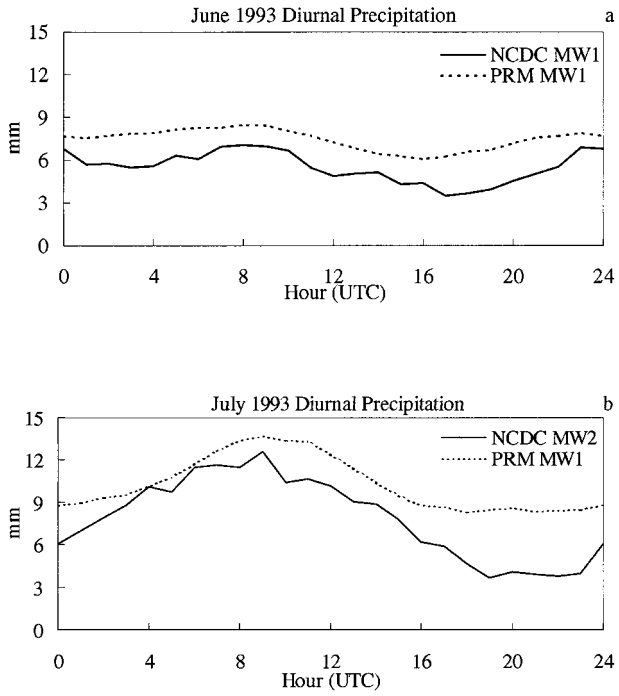

FIG. 7. As in Fig. 6 except that the data are integrated by hour of the day.

tive model and observed maximum regions denoted in Fig. 1).

Figure 6 demonstrates some of the differences between the June and July periods. The Midwest averaged daily precipitation of the June control simulation exhibits a similar periodicity (~5 days) of the precipitation events that occurred during June 1993. While the magnitude of the events tends to be overestimated, the model reproduces the precipitation associated with the cyclone events and their passage across the region. The locations of the July modeled and observed daily averages (Fig. 6b) are centered on the respective centers of heaviest precipitation in order to investigate the temporal variability of precipitation (recognizing the discrepancy in location of precipitation maxima). The essence of this graph is not intended to directly compare the magnitude of precipitation in the different regions but rather to compare the relative frequency of the occurrence of precipitation within the respective centers of maximum precipitation. During July, significant precipitation events occurred on most days of the month. While the model does not reproduce each event precisely, the pattern of the events has remarkable similarities to the observations. Figure 6 shows that the model is capable of reproducing the different precipitation processes associated with the different weather systems in each month.

Examination of the diurnal precipitation shows some differences between June and July (Fig. 7). The model generally overestimates the precipitation at each hour for the June 1993 simulation; however, the model's diurnal trace exhibits a pattern similar to the observations. During July, the model shows a strong diurnal oscillation, similar to the observations, and a maximum value at 0900 UTC. The largest discrepancy between model and observation during July, however, is focused during the afternoon hours. While the model tends to overestimate the precipitation, both the diurnal and daily traces of precipitation in the Midwest for both June and July show patterns similar to the observed traces.

Overall, the PRM control simulations include many of the observed atmospheric features that occurred during the summer of 1993 and especially those directly related to the heavy precipitation. The model was able to reproduce the monthly mean large-scale atmospheric circulation and heavy precipitation, as well as the differences between June and July. In particular, the PRM precipitation in June shows a similar periodicity in the Midwest compared to observations, which is related to the passage of synoptic-scale cyclones, while in July, almost every day showed some precipitation and larger diurnal oscillation.

Of course, the model does have some differences when compared to observations. Most notably, area-averaged precipitation is overestimated (25% in June and 30% in July). While the focus of the modeled precipitation in July is shifted northward, the atmospheric circulation that generates the precipitation is consistent with observational analyses. The verisimilitude of the model simulations permits the subsequent sensitivity experiments, which are used to evaluate the interaction between the surface and precipitating systems.

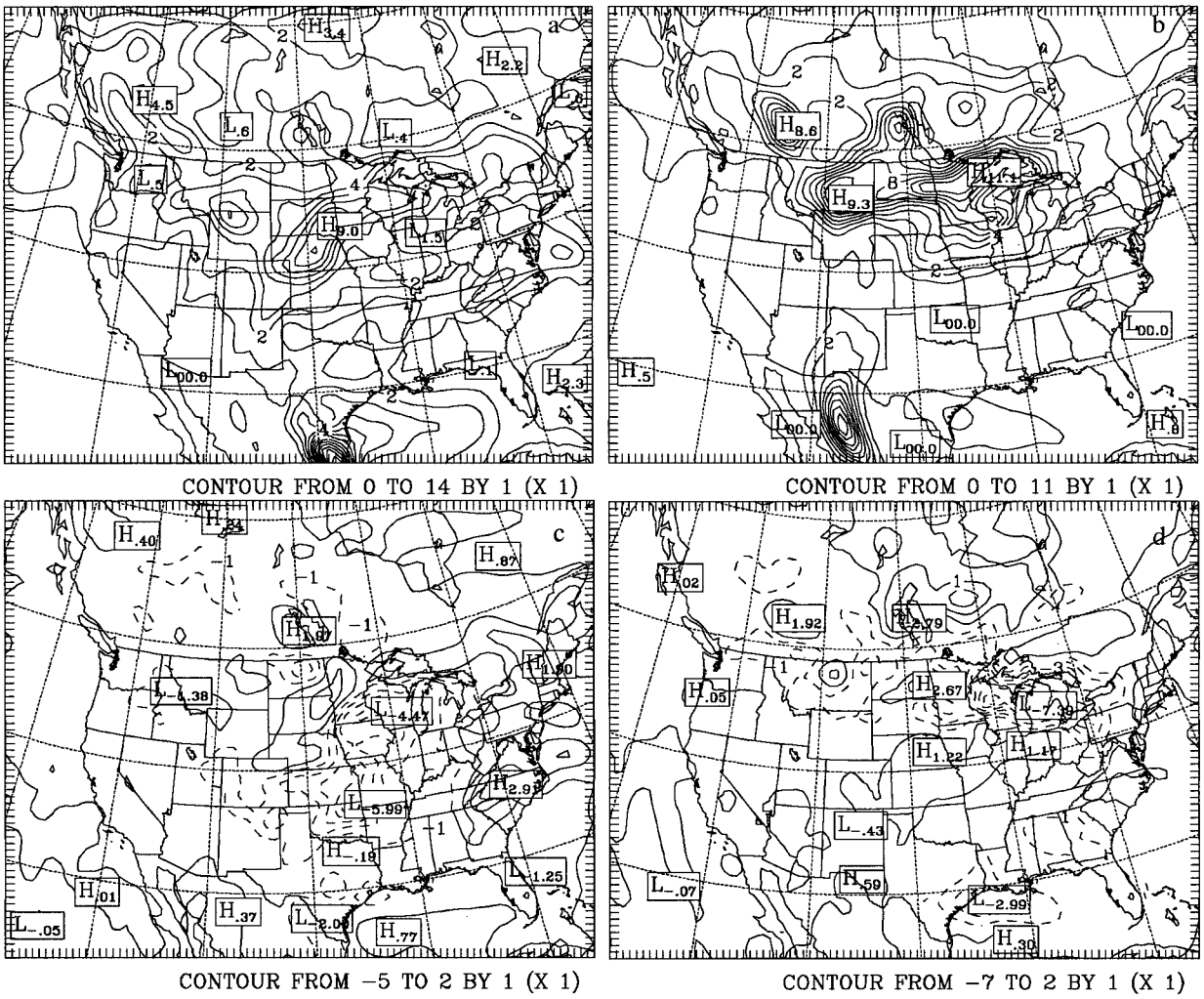

FIG. 8. The differences of total precipitation between case 1 and the control simulations of (a) Jun and (b) Jul. The unit are mm day^{-1}.

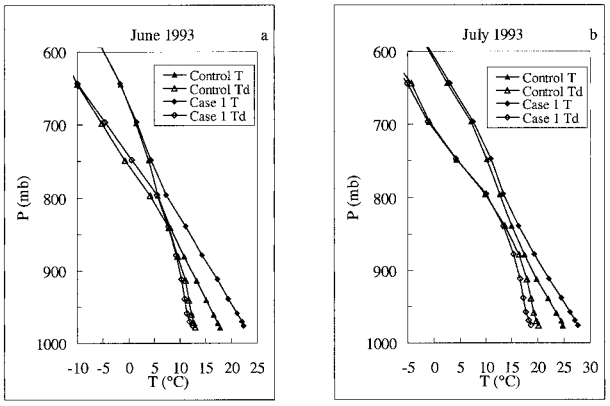

FIG. 9. 0000 UTC monthly mean profiles of temperature and dewpoint temperature within the MW1 region for the case 1 and control simulations of (a) Jun and (b) Jul.

4. Sensitivity simulations

As discussed in previous sections, studies of the influence of soil water on the July precipitation have yielded differing results. In Beljaars et al. (1996), low evaporation upstream from the precipitation maximum caused a substantial PBL capping inversion that prohibited convection and reduced precipitation in the flood region. The results of Paegle et al. (1996), however, show that for uniform, high evaporation upstream from the precipitation, the atmospheric PBL temperature becomes colder and the diurnal oscillation of the LLJ is reduced. The weaker nocturnal LLJ causes less moisture convergence downstream and, hence, less precipitation. It is difficult to compare these results because they are determined with two different experimental platforms. Therefore, similar sensitivity experiments were performed with the PRM in order to identify any physical reasons for the different results.

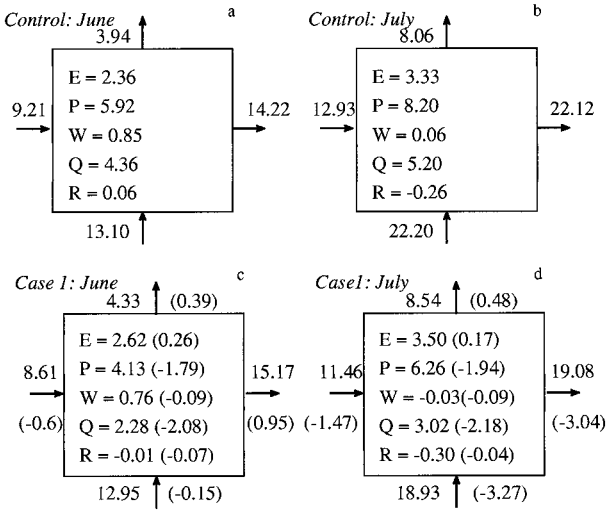

FIG. 10. MW1 region monthly hydrology budgets for control (a) Jun and (b) Jul, and for case 1 (c) Jun and (d) Jul. The symbols are defined in the appendix. The units are mm day^{-1}, the arrows indicate the transport direction (and sign), and the differences from the control are indicated in parentheses.

a. Case 1: Dry soil at all land points

To generate the case 1 soil moisture anomaly, the control soil water is reduced to the wilting point water content at all land points, except where it is already less than the wilting point (generally, the arid southwest). The initial perturbation is imposed throughout the soil column (1 m deep). The soil moisture was still predicted, as in the control simulations, but the soil moisture anomalies generally persisted throughout the 30-day period. Comparing the precipitation of case 1 and the control shows that the soil moisture anomaly reduced both the area and magnitude of the heaviest June rainfall (Fig. 8). The differences of total precipitation can be very large near the central precipitation maximum ($\sim$4 mm day^{-1} in June and $\sim$7 mm day^{-1} in July). While the June case does indicate a reduction of precipitation over the upper Mississippi River basin, there were some increases in precipitation to the west. Note that in June, the south-central United States also experiences a strong decline in precipitation. In July, the reduction of precipitation is focused near the maximum of control precipitation. Gulf coastal precipitation is also affected by the soil moisture anomaly.

Beljaars et al. (1996) results suggest that the thermodynamic stability was greatly reduced by the presence of drier soil. This was supported by a strong temperature inversion at the top of the PBL that formed and prohibited the development of deep convection in their dry case. At 0000 UTC, the case 1 lapse rates in both months are larger than the control due to the warmer surface temperature and increased dry convection (Fig. 9). The profiles in each month are warmer and slightly drier than the control. Moist convective instability is, in general, less than the control; however, the large capping inversion noted by Beljaars et al. (1996) does not occur in case 1.

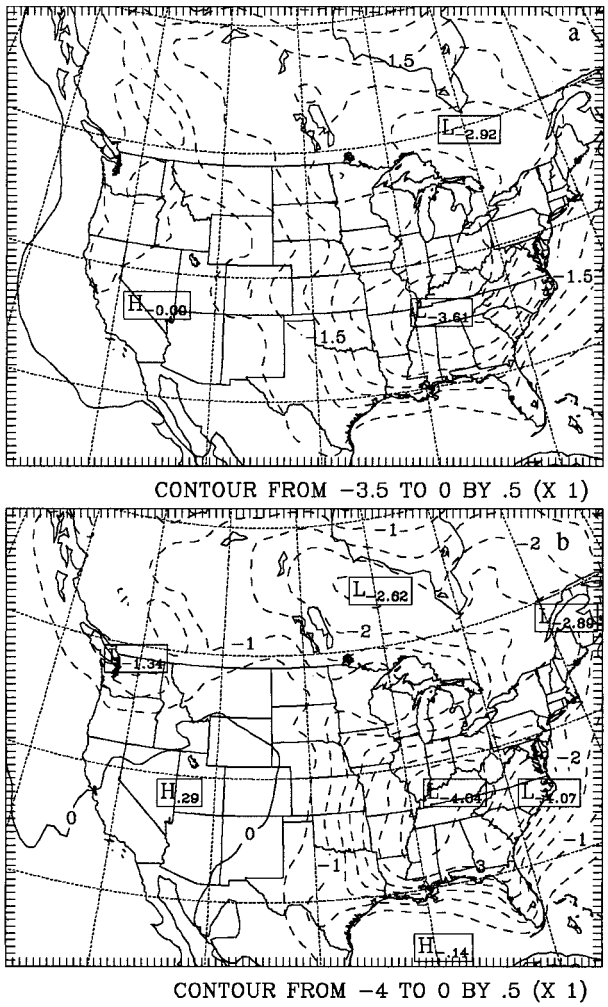

FIG. 11. Monthly mean differences of mean sea level pressure, case 1 − control (interval 0.5 mb) for (a) Jun and (b) Jul.

The area-averaged hydrology budgets for the MW1 region (see Fig. 1) are presented in Fig. 10. The appendix discusses the development and calculations of the model hydrology budget. Precipitation has been strongly affected by the soil moisture anomaly, and the difference is balanced mainly by the reduction of moisture convergence (in a time-averaged sense). In each simulation, June and July, the change of precipitation (area averaged) is approximately -2 mm day^{-1}, but the percent change is 30% and 24%, respectively. The reduction of moisture convergence is just slightly larger than 2 mm day^{-1}. The transport of water through the MW1 boundaries exhibits some monthly variations. During June, the inflow transport is slightly decreased, while the outflow of moisture is increased, resulting in a net reduction of moisture convergence. In July, however, both the total inflow and outflow are reduced with a net reduction in moisture convergence.

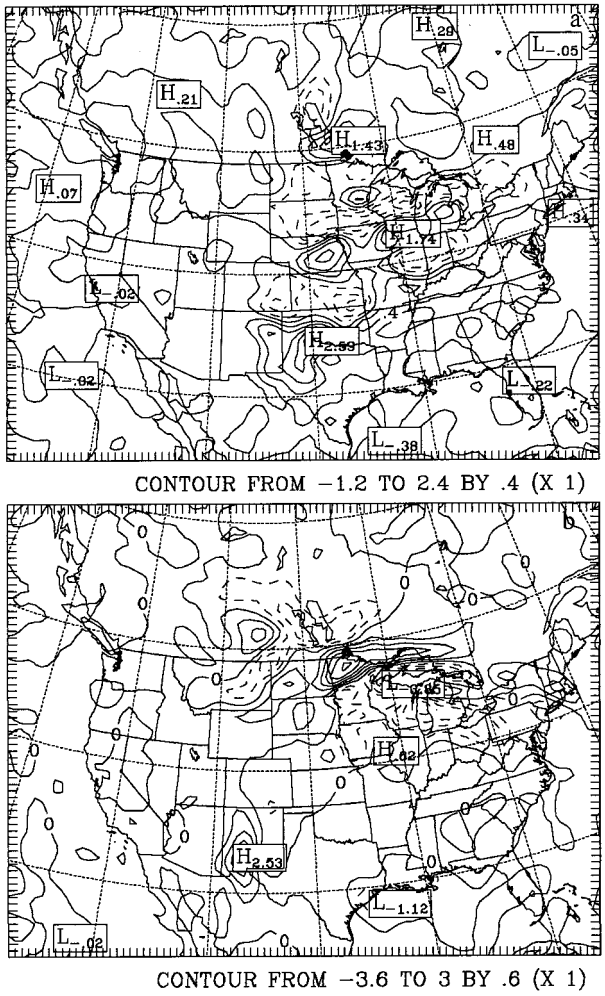

FIG. 12. The differences of total precipitation, case 2A − control for (a) Jun (interval 0.4 mm day^{-1}) and (b) Jul (interval 0.6 mm day^{-1}).

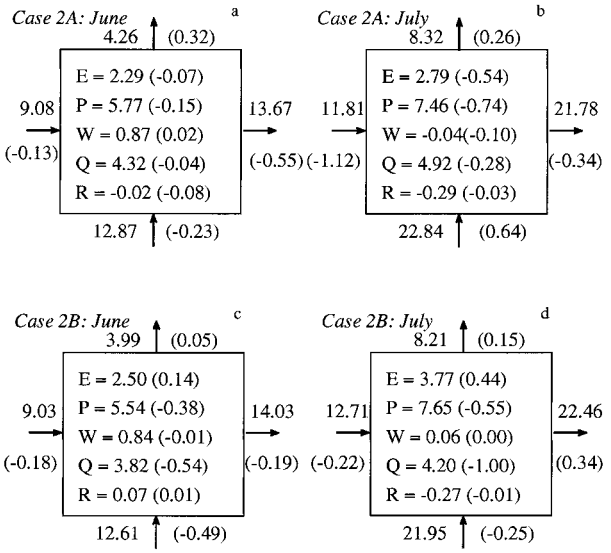

FIG. 13. MW1 region monthly hydrology budgets for case 2A (a) Jun and (b) Jul, and for case 2B (c) Jun and (d) Jul. Symbols are defined in the appendix. Units are mm day^{-1}, arrows indicate the transport direction and sign, and differences from control are in parentheses.

The dry soil anomaly causes an increase in the heating of the land surface, which leads to lower surface pressure over the land (Fig. 11). The pressure differences are centered over the southern part of the Midwest region. The lower surface pressure is strategically located so that the pressure gradient in the lower troposphere near the LLJ region is lessened, thereby reducing the meridional wind by 10% in June and 15% in July. This feedback process has been linked to the perpetuation of drought conditions in the United States (Namias 1982; Oglesby and Erickson 1989; Oglesby 1991). Therefore, the low-level large-scale circulation anomaly, coupled with the variation of the thermodynamic stability, are very influential in reducing the large-scale moisture convergence and precipitation.

b. Case 2: Soil moisture in the southern Great Plains

Case 2 contrasts case 1, in that the soil moisture anomaly is imposed over a subregion of the model domain. The case 2A initial soil moisture over the southern Great Plains (SGP in Fig. 1) is increased to the field capacity (the amount of water that causes the ground surface evaporation to occur at its potential rate). While this increases the evaporation, as in Paegle et al. (1996), the soil moisture is predicted after the initial time, whereas Paegle et al. (1996) used fixed diurnal evaporation. For the July case, SGP evaporation is increased by 50% over the control regional evaporation but by only 20% during June.

The precipitation is affected, but the trend in the horizontal difference field is not necessarily clear (Fig. 12). In June, there is a local (SGP region) increase in precipitation, but downstream from the SGP region there are mixed positive and negative precipitation anomalies. During July, the largest decline in precipitation occurs in the Midwest (~3.8 mm day^{-1}) near the heaviest control precipitation, but there also appears to be a shift in the precipitation, resulting in increased precipitation to the northwest. As suggested by Paegle et al. (1996), however, the area-averaged MW1 precipitation was decreased in the wet anomaly case (Figs. 13a and 13b). The results are still somewhat weaker during June. In general, there is a decrease in the transport of water into the region, but southerly flow actually increases in July. The lessening of precipitation, especially in July, is related to a reduction in the intensity of the LLJ (by approximately 15%), mostly during the nighttime hours (Fig. 14). Note that, again, the response in June is not as prominent as in July. This may be due to the transient nature of the June circulations and the associated weaker monthly mean patterns.

Case 2B contrasts case 2A by decreasing the soil

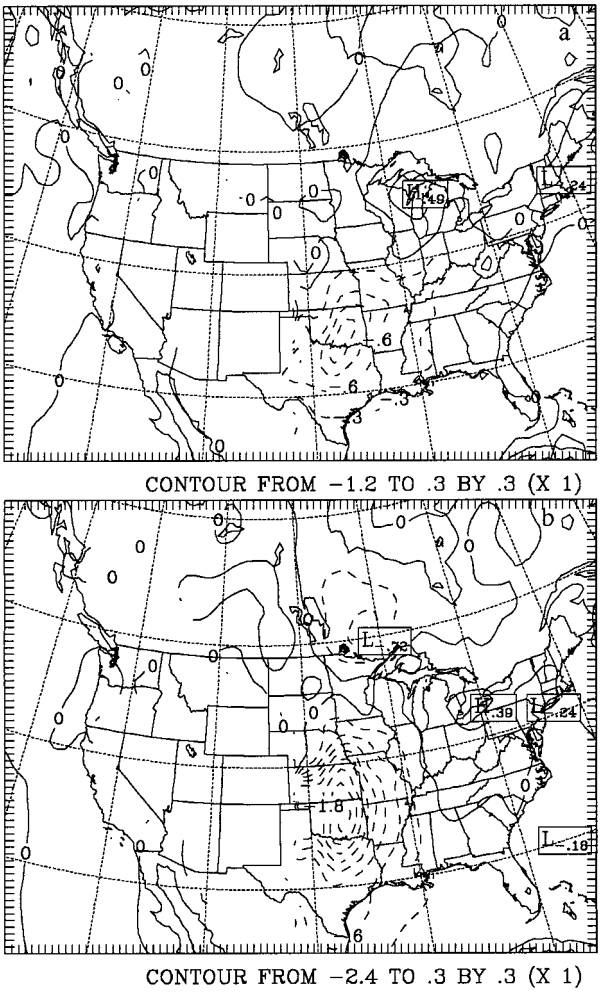

FIG. 14. Monthly mean difference, case 2A − control of the meridional wind component (interval 0.3 m s^{-1}), 1000 m above sea level averaged at 0600 UTC for (a) Jun and (b) Jul.

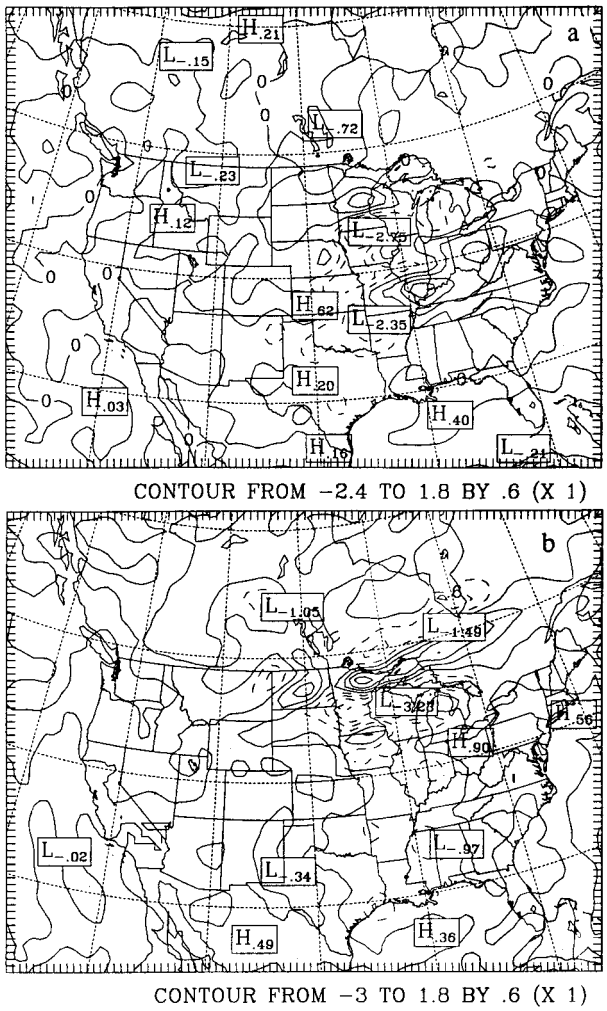

FIG. 15. The differences of total precipitation, case 2B − control (interval 0.6 mm day^{-1}) for (a) Jun and (b) Jul.

water content to its wilting point. Paegle et al.'s results suggest that the precipitation should increase, because of the stronger diurnal oscillations in lower-tropospheric temperature and the LLJ. Here, the response of the precipitation has a certain amount of variability, but the maximum of precipitation is mostly reduced (Fig. 15). The PRM hydrology budgets (Figs. 13c and 13d) indicate a reduction in moisture convergence and precipitation in the MW1 region. It is also interesting to note the variations in evaporation in case 2, which are a result of the changes in lower-tropospheric specific humidity.

In the July control simulations, a strong gradient of soil moisture occurs in the SGP region (Fig. 16a), where western Texas and New Mexico are dry, and eastern Texas is quite moist. This leads to differential heating across the SGP region (Fig. 16b). Due to precipitation in the western SGP region in June, the June differential heating is weaker (figure not included). In both cases 2A and 2B, the soil moisture gradient is removed and the surface heating becomes more uniform. In case 2A the wet eastern SGP leads to cooler temperatures and higher mean sea level pressure, and it reduces the surface pressure gradient and the LLJ (Fig. 17a). The dry case 2B, on the other hand, leads to warmer temperature and lower sea level pressure in the western SGP, and again, the pressure gradient and LLJ are reduced (Fig. 17b). Therefore, the gradient of surface soil moisture and consequent differential heating enhance the pressure gradient and LLJ in the SGP region. Similar results have been discussed by McCorkle (1988) (studying the diurnal variation of the LLJ) and Sun and Wu (1992) (studying the secondary circulation and the LLJ around the west Texas dryline). While these processes are present in June, the monthly mean anomalies tend to be weaker than in July.

5. Summary and conclusions

During the summer of 1993, persistent and heavy precipitation caused a long-lived catastrophic flood in

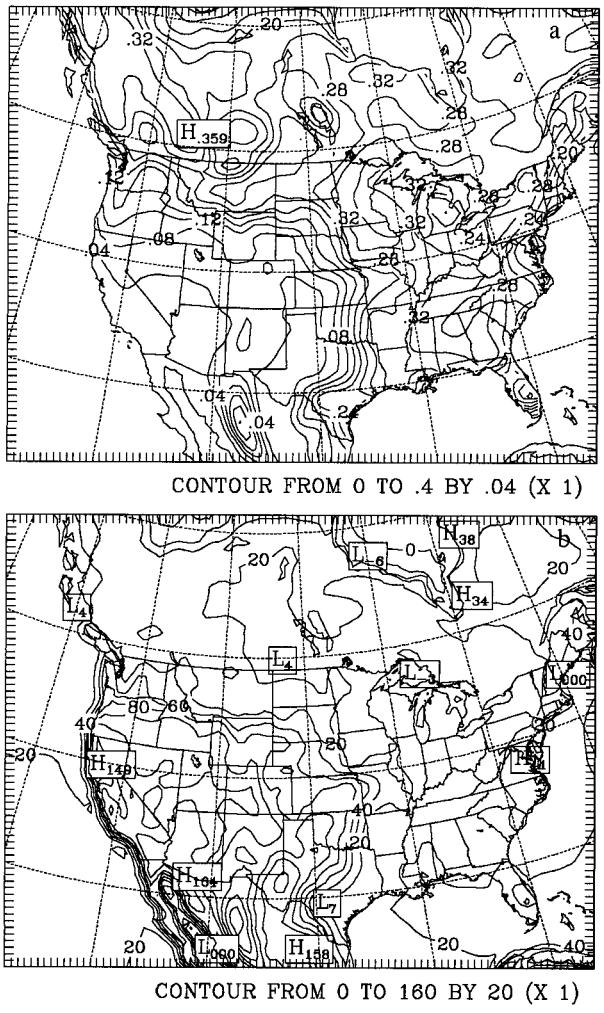

FIG. 16. July control simulation monthly mean (a) surface soil water content (interval 0.04 m^3 m^{-3}) and (b) surface sensible heat flux (interval 20 W m^{-2}).

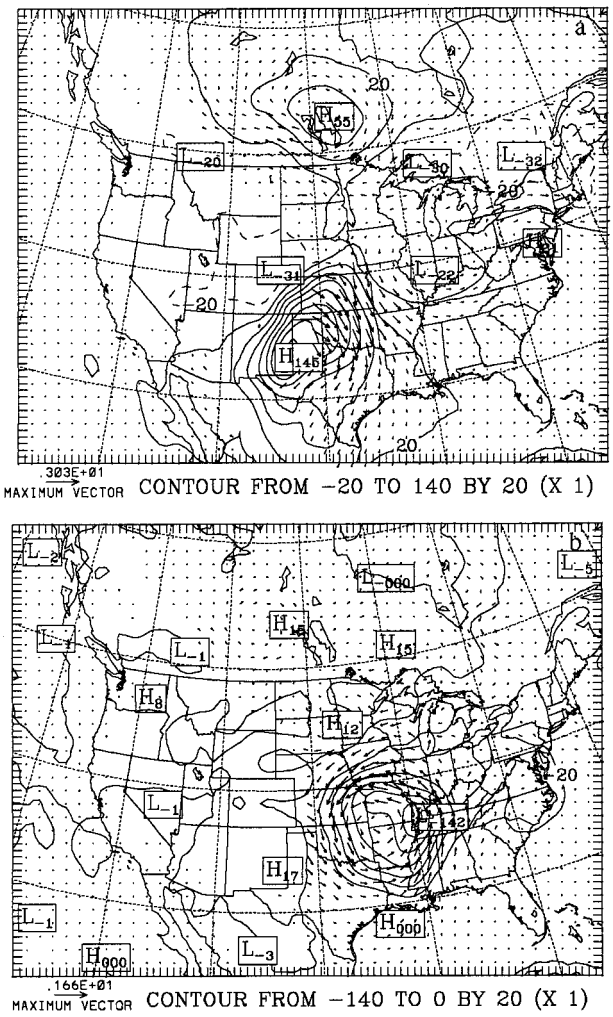

FIG. 17. Monthly mean Jul mean sea level pressure differences (interval 20 Pa) and wind vectors at 1000 m above sea level (0600 UTC average) for (a) case 2A and (b) case 2B. Note that (b) negative contours are not dashed.

the midwestern United States. In this paper, Midwest hydrology, atmospheric circulation of the 1993 summer, and feedback between the surface and precipitating systems were investigated using the Purdue Regional Model (PRM). Due to the differences between each month, both June and July were included in the experimentation. Careful consideration of the observed features prompted the use of a large model domain, which allows the model to develop critical components of the weather systems as independently as possible. In particular, the Great Plains and Midwest regions were placed near the center of the model domain, sufficiently far from lateral boundary forcing so that the model prognostic equations controlled the local weather systems, anomalous precipitation, and LLJ.

The PRM control simulations reproduced the large-scale atmospheric features that characterized the summer of 1993. Specifically, the upper-level jet stream and trough over the northwestern United States were present in control cases, as well as the LLJ, general pattern of moisture transport, and heavy precipitation in the Midwest. The daily precipitation record (area averaged over the heaviest rainfall) indicated that the model also developed the evolution and periodicity of the precipitation events comparable with the observations and correctly reproduced the differences between June and July.

While the PRM simulated transient cyclones and their precipitation well, the location of the mesoscale convective precipitation systems during July was shifted to the north. In addition, control simulations yielded an overestimation of precipitation (25%–30%, at the central maximum). The modeled circulation is, otherwise, consistent with the observations, in that the heavy precipitation is directly related to convergence associated with the LLJ and to the upper-level longwave circulation. For these circumstances, conclusions regarding the coupling of the LLJ and the precipitation should be

robust. However, the influence of the Gulf of Mexico may not be well represented due to the difference in proximity.

The sensitivity of the LLJ, planetary boundary layer, and heavy precipitation were examined by imposing various soil moisture and surface anomalies in the model simulation. A dry soil anomaly that covered the entire domain generally decreased the moist convective instability of the PBL, but not as much as in Beljaars et al. (1996). The increased surface heating induced a large-scale surface pressure perturbation (centered in the southeastern United States) that weakened the LLJ and moisture transport, similar to Oglesby and Erickson's (1989) results for drought cases.

Paegle et al. (1996) and Beljaars et al. (1996) proposed different mechanisms to enhance or reduce the Midwestern precipitation that depend on whether the soil is wet or dry. Here, the moist SGP anomaly reduced the intensity of the LLJ and the heaviest precipitation (as suggested by Paegle et al. 1996), but the corresponding dry soil anomaly also reduced the LLJ and precipitation (similar to Beljaars et al. 1996). However, both sensitivity simulations exhibited some similar responses in the low-level atmospheric circulation. The control simulations (especially for July) had a strong gradient of soil moisture in the southern Great Plains. This leads to differential heating and a secondary circulation that enhance the LLJ. By imposing uniform soil moisture, either wet or dry, the differential heating is eliminated. The pressure gradient near the LLJ and the moisture convergence are reduced. Therefore, less precipitation occurs downstream. The monthly mean June LLJ was weaker than July and the sensitivity to the surface anomalies was also less than July. McCorkle (1988) and Sun and Wu (1992) have documented similar responses of the modeled LLJ on shorter timescales.

Acknowledgments. The authors would like to recognize the efforts of Drs. Philip Smith, Dayton Vincent, and Robert Oglesby in reviewing and critiquing this work as part of the first author's Ph.D. dissertation (Bosilovich 1997). The suggestions and comments by this paper's anonymous reviewers greatly improved the final draft. We are grateful for Dr. Jiun-dar Chern's work in refining the PRM code, which greatly improved the efficiency of performing these experiments. Drs. Jiun-dar Chern and Patrick Haines, and Ms. Shu-hua Chen provided many useful discussions throughout the development of these experiments. We would like to express our appreciation to Mr. Jim Gardner for proofreading this manuscript and his many years of service to the Department of Earth and Atmospheric Science. ECMWF operational analyses and NCDC hourly precipitation (TD-3240) were obtained through the NCAR data archive. The enormous computer resources needed to carry out the experiments were provided by The IBM Center for Environmental Research at Purdue University, directed by Dr. Joe Sarsenski. The National Science Foundation under Grant ATMS-9213730 and the Purdue Research Foundation supported this work.

APPENDIX

PRM Atmospheric Hydrology

In this study, the model's hydrology budget is investigated in detail. In this section, the model's hydrology budget is derived and the important terms are discussed. The model continuity equation (in sigma coordinates) is written as

$$\frac{\partial p_*}{\partial t} = -\nabla_3(p_* \mathbf{V}_3), \tag{A1}$$

where p_* is the total pressure of the column (surface pressure minus top pressure), and $\mathbf{V}_3$ is the three-dimensional wind vector. The prognostic equation for water vapor is

$$\frac{\partial q}{\partial t} = -\mathbf{V}_3\nabla_3 q + S + D, \tag{A2}$$

where q is the specific humidity, S represents all the external sources and sinks of water vapor, and D is the diffusion of water vapor. By multiplying (1) by q and (2) by p_*, and combining the resulting equations, the divergent form of the hydrology equation is written as

$$\frac{\partial p_* q}{\partial t} = -\nabla_3(p_* q \mathbf{V}_3) + p_* S + p_* D. \tag{A3}$$

Equation (3) is then vertically integrated in the model's sigma coordinate system (and divided by gravity),

$$\begin{aligned} g^{-1} \int_0^1 \frac{\partial p_* q}{\partial t}\, d\sigma \\ = -g^{-1} \int_0^1 \nabla_3(p_* q \mathbf{V}_3)\, d\sigma + g^{-1} \int_0^1 p_* S\, d\sigma \\ + g^{-1} \int_0^1 p_* D\, d\sigma. \end{aligned} \tag{A4}$$

To simplify the presentation of the atmospheric hydrology budget, the terms of the equation are represented by the following notation:

$$W = g^{-1} \int_0^1 \frac{\partial p_* q}{\partial t}\, d\sigma, \tag{A5}$$

$$Q = -g^{-1} \int_0^1 \nabla_3[p_* q \mathbf{V}]\, d\sigma, \tag{A6}$$

$$E - P = g^{-1} \int_0^1 p_* S\, d\sigma, \tag{A7}$$

$$R = g^{-1} \int_0^1 p_* D\, d\sigma. \tag{A8}$$

Here W is the total change of precipitable water. In general, it is a small term, but not small enough to neglect from a monthly hydrology budget. Here Q is the vertically integrated atmospheric moisture convergence. To ensure the accuracy of the regional hydrology budget, Q is integrated at the model time step. Vertical integration of all the sources and sinks of water vapor in the column yields the difference of surface evaporation (E) and precipitation that reaches the surface (P). The model includes a numerical routine for diffusion of water vapor (R). For this study, the diffusion term of a regional hydrology budget is simply solved for as a residual of the other terms in the equation. In this way, diffusion is combined with convergence of liquid and solid water into one term. By replacing the terms of (4) with the abbreviated notation, the model's atmospheric hydrology budget is given by

$$W = Q + E - P + R. \tag{A9}$$

When examining the regional area-averaged hydrology budgets, it is also useful to identify the boundary fluxes. By applying the divergence theorem to the moisture convergence term of (3) [also see Eq. (6)], the transport of water vapor can be used to compute the boundary fluxes of water vapor. It is important to note that, for this study, instantaneous 6-h data are used to compute the moisture transport. The line integration can be used to estimate the moisture convergence, but because of the large time interval, the convergence may have more error than Q [in Eq. (6)]. The two computations of moisture convergence are not necessarily the same.

REFERENCES

Beljaars, A. C. M., P. Viterbo, M. Miller, and A. Betts, 1996: The anomalous rainfall over the United States during July 1993: Sensitivity to land surface parameterization and soil moisture anomalies. *Mon. Wea. Rev.,* **124,** 362–383.

Bell, G. D., and J. E. Janowiak, 1995: Atmospheric circulation associated with the Midwest floods of 1993. *Bull. Amer. Meteor. Soc.,* **76,** 681–695.

Betts, A., J. Ball, A. Beljaars, M. Miller, and P. Viterbo, 1994: Coupling between land surface, boundary layer parameterizations and rainfall on local and regional scales: Lessons from the wet summer of 1993. Preprints, *Fifth Symp. on Global Change Studies*, Nashville, TN, Amer. Meteor. Soc., 174–181.

Bosilovich, M. G., 1997: Numerical simulation of the 1993 Midwest flood. Ph.D. dissertation, Purdue University, West Lafayette, IN, 122 pp. [Available from Purdue University, West Lafayette, IN 47907.]

——, and W.-Y. Sun, 1995: Formulation and verification of a land surface parameterization for atmospheric numerical models. *Bound.-Layer Meteor.,* **73,** 321–341.

——, and ——, 1998: Monthly simulation of surface layer fluxes and soil properties during FIFE. *J. Atmos. Sci.,* **55,** 1170–1184.

Chen, T.-C., and J. Kpaeyeh, 1993: The synoptic scale environment associated with the low level jet of the Great Plains. *Mon. Wea. Rev.,* **121,** 416–420.

Chern, J.-D., 1994: Numerical simulations of cyclogenesis over the western United States. Ph.D. dissertation, Purdue University, West Lafayette, IN, 178 pp. [Available from Purdue University, West Lafayette, IN 47907.]

Davies, H. C., 1976: Limitations of some common lateral boundary schemes used in regional NWP models. *Quart. J. Roy. Meteor. Soc.,* **102,** 405–418.

Deardorff, J. W., 1978: Efficient prediction of ground surface temperature and moisture with inclusion of a layer of vegetation. *J. Geophys. Res.,* **83** (C4), 1889–1903.

Giorgi, F., L. Mearns, C. Shields, and L. Mayer, 1996: A regional model study of the importance of local versus remote controls of the 1988 drought and the 1993 flood over the central United States. *J. Climate,* **9,** 1150–1162.

Hsu, W.-R., and W.-Y. Sun, 1991: Numerical study of mesoscale cellular convection. *Bound.-Layer Meteor.,* **57,** 167–186.

——, and ——, 1994: A numerical study of a low-level jet and its accompanying secondary circulation in a Mei-Yu system. *Mon. Wea. Rev.,* **122,** 324–340.

Jones, R., J. Murphy, and M. Noguer, 1995: Simulation of climate change over Europe using a nested regional climate model. Part I: Assessment of control climate, including sensitivity to location of lateral boundaries. *Quart. J. Roy. Meteor. Soc.,* **121,** 1413–1449.

Kunkel, K. E., S. Chagnon, and J. Angel, 1994: Climatic aspects of the 1993 upper Mississippi River basin flood. *Bull. Amer. Meteor. Soc.,* **75,** 811–822.

Maddox, R. A., 1983: Large-scale meteorological conditions associated with midlatitude mesoscale convective complexes. *Mon. Wea. Rev.,* **111,** 1475–1493.

McCorkle, M. D., 1988: Simulation of surface-moisture effects on the Great Plains low-level jet. *Mon. Wea. Rev.,* **116,** 1705–1720.

Min, W., and S. Schubert, 1997: The climate signal in regional moisture fluxes: A comparison of three global data assimilation products. *J. Climate,* **10,** 2623–2642.

Mintz, Y., 1984: *Global Climate.* Cambridge, 233 pp.

Mo, K. C., J. Nogues-Paegle, and J. Paegle, 1995: Physical mechanisms of the 1993 summer floods. *J. Atmos. Sci.,* **52,** 879–895.

Molinari, J., 1982: A method for calculating the effects of deep cumulus convection in numerical models. *Mon. Wea. Rev.,* **110,** 1527–1534.

Namias, J., 1982: Anatomy of Great Plains protracted heat waves (especially the 1980 U.S. summer drought). *Mon. Wea. Rev.,* **110,** 824–838.

Oglesby, R. J., 1991: Springtime soil moisture, natural climatic variability and North American drought as simulated by the NCAR Community Climate Model 1. *J. Climate,* **4,** 890–897.

——, and D. Erickson, 1989: Soil moisture and persistence of North American drought. *J. Climate,* **2,** 1362–1380.

Paegle, J., K. C. Mo, and J. Nogues-Paegle, 1996: Dependence of simulated precipitation on surface evaporation during the 1993 United States summer floods. *Mon. Wea. Rev.,* **124,** 345–361.

Philip, J. R., 1957: Evaporation, moisture and heat fields in the soil. *J. Meteor.,* **14,** 354–361.

Roads, J. O., S.-C. Chen, A. K. Guetter, and K. P. Georgakakos, 1994: Large-scale aspects of the United States hydrologic cycle. *Bull. Amer. Meteor. Soc.,* **75,** 1589–1610.

Sellers, P. J., Y. Mintz, Y. Sud, and A. Dalcher, 1986: The design of a Simple Biosphere Model (SiB) for use within general circulation models. *J. Atmos. Sci.,* **43,** 505–531.

Seth, A., and F. Giorgi, 1997: A regional climate model study of the role of soil moisture in the extreme events of 1988 and 1993 in the central United States. Preprints, *13th Conf. on Hydrology,* Long Beach, CA, Amer. Meteor. Soc., 78–79.

Sun, W.-Y., 1993a: Numerical experiments for advection equation. *J. Comput. Phys.,* **108,** 264–271.

——, 1993b: Numerical simulation of a planetary boundary layer. Part I: Cloud-free case. *Contrib. Atmos. Phys.,* **66,** 3–16.

——, 1995: Pressure gradient in a sigma coordinate. *TAO,* **6,** 579–590.

——, and C.-Z. Chang, 1986a: Diffusion model for a convective layer. Part 1: Numerical simulation of a convective boundary layer. *J. Climate Appl. Meteor.,* **25,** 1445–1453.

——, and ——, 1986b: Diffusion model for a convective layer. Part

II: Plume released from a continuous point source. *J. Climate Appl. Meteor.*, **25,** 1454–1463.
——, and A. Yildirim, 1989: Air mass modification over Lake Michigan. *Bound.-Layer Meteor.*, **48,** 345–360.
——, and C.-C. Wu, 1992: Formation and diurnal variation of the dryline. *J. Atmos. Sci.*, **49,** 1606–1619.
——, and J.-D. Chern, 1993: Diurnal variation of lee-vortexes in Taiwan and surrounding area. *J. Atmos. Sci.*, **50,** 3404–3430.
——, and ——, 1994: Numerical experiments of vortices in the wake of idealized large mountains. *J. Atmos. Sci.*, **51,** 191–209.
——, and M. G. Bosilovich, 1996: Planetary boundary layer and surface layer sensitivity to land surface parameters. *Bound.-Layer Meteor.*, **77,** 353–378.
——, J.-D. Chern, C.-C. Wu, and W.-R. Hsu, 1991: Numerical simulation of mesoscale circulation in Taiwan and surrounding area. *Mon. Wea. Rev.*, **119,** 2558–2573.
Trenberth, K. E., and C. J. Guillemot, 1996: Physical processes involved in the 1988 drought and 1993 floods in North America. *J. Climate*, **9,** 1288–1298.
Uccellini, L., 1980: On the role of upper tropospheric jet streaks and leeside cyclogenesis in the development of low-level jets in the Great Plains. *Mon. Wea. Rev.*, **108,** 1689–1696.